Characterization of Free-space Gaussian Beam Propagation and Recent Developments of FSO Communication Technology: A Review

Joseph George Chalil[1], Shachi Kadam[2], Chinchu Joseph[3], K.J. Kulkarni[2], A.A.Bazil Raj[3]

[1] Department of Electronics Science, Fergusson College, Pune, Maharashtra, 411004

[2] Electronics and telecommunication, Pune Vidyarthi Girha's College of Engineering and Technology and G.K. Patel (Wani) Institute of Management, Vidyanagari, Parvati, Pune, Maharashtra, India,411009

[3] RF Photonics Laboratory, Defence Institute of Advanced Technology, Girinagar, Pune, Maharashtra, India, 411025

Abstract: **In typical scenarios, the laser beam diverges significantly when transitioning from the fiber into free space. To minimize divergence in wide range Wireless Optical Communication (WOC) applications and extend the potential link range, the impact of beam spread is reduced by collimating the beam using an appropriate collimating lens positioned from the transmission fiber endpoint at its focal length. The beam is refocused back into the fiber using a comparable lens close to the receiving fiber end point. This report delves into the concepts relevant for studying a similar free-space optical communication system and theoretically optimizing the received beam spot size to ensure maximum efficiency of the received data signal. It's crucial to consider atmospheric conditions when studying a real system due to their significant impact. Also the recent advancements and developments have been reviewed and discussed in this work.**

Keywords: **Free Space Optical Communication, Beam divergence, Gaussian beam, beam stability, Error correction.**

1.   INTRODUCTION

Using laser sources, FSO (Free Space Optics) is a line-of-sight communication method that establishes optical bandwidth links. This optical communication method uses light propagation in open space, such as air or vacuum, to wirelessly transfer data for computer networking and telecommunication applications. Studies on the Free Space Optical Communication (FSOC) technology date back many years [1]. The development of tap-proof communication systems and high-speed information transmission has become a trend in modern communication structures. These systems are useful in links involving satellites, deep-space probes, ground stations, unmanned aerial vehicles (UAVs), high altitude platforms (HAPs), aircraft, and other similar communication networks. As bandwidth, spectrum and security issues favour it as a supplement to the radio frequency (RF) communication, FSO is the next frontier for net-centric connectivity [2].

Within the FSO, access points are linked via coaxial and microwave/radio frequency (RF) cables. The constraints of these communication lines, which are often copper and RF-based, include poor bandwidth, high deployment costs, unsecure data transmission, and expensive licensing. Optical fiber communication though have high data transmission rate (>10 Gbps) at 0.2 dB/km attenuation, it is mostly used for optical backbone networks [3]. Since free-space optical (FSO) communication uses light waves to transfer a large amount of data, it is a viable solution to the last-mile bottleneck problem.FSO communication means to send information through unguided propagation medium by the use of optical frequencies, i.e., infrared (IR), visible, and ultraviolet (UV) band [4].

Bandwidth scalability, speed of deployment, and cost effectiveness are some advantages why FSO is considered to be an optimal solution in terms of optical wireless communication technology [5]. Long range (tens of kilometers) or short range (a few meters) can be achieved using terrestrial FSO lines. Short-distance connections by interconnecting local area network segments housed in buildings provide high-speed connectivity to end users. Long-range FSO communication links extend up to existing metropolitan area fibre rings or to connect new networks, extending their services to core infrastructure [6]. Free space fiber communications (Fsoc) is an age-long technology that entails the transmission of information-laden optical radiation through the free-space channel [7]. FSOC technology is one of the most promising alternative schemes for addressing the 'last mile' bottleneck in the emerging broadband access markets [8]. Terrestrial point-to-point free space optical (FSO) communication systems are operated at visible light (VL), infrared (IR), or ultraviolet (UV) spectrum frequencies [9]. Narrow, concentrated light beams from a laser diode at the transmitter are utilized to create high-data-rate communication channels between a transmitter and a receiver. The system provides communication between two fixed points over distances ranging from a few nm to several thousand kilometres [10].

While fixed FSO links between buildings have long been established and today form a separate commercial product segment in local and metropolitan area networks, the mobile and long-range applications of this technology need extreme pointing and tracking accuracy because of the small optical beam divergences involved [11]. To use the FSOC technology to the fullest, similar challenges need to be addressed and studied upon.

1.1. Brief history of FSO

According to history, light was used in the early days of optical wireless communication. The ancient people reflected light from the sun using polished shields and communicate some pre-coded information. The actual concept of FSO was taken into consideration in the 8th century [12]. Fire beacon was used for alphabetic signalling in the coded form by the ancient Greeks with torches developed by Polybius, Democleitus and Cleoxenus [13] to inform their recipients. Carl Friedrich Gauss [14] developed a heliograph mechanism using twin mirrors to direct a controlled beam of sunlight in 1810. The first FSO photo-phone concept was practically demonstrated by Alexander Graham Bell [15,16], who is the pioneer of FSO communication. On June 3, 1880, he experimented with wirelessly transmitting voice over a beam of light through the air, about 213 meters apart. He called this project a "photo-phone," but his invention was never put into practice commercially. However, decades later, the idea was implemented in military communication telegraphy, where three different types of transmitters based on optical Morse, called Blinkgerat [17], were used by German signals for distances up to 4 km during the day and up to 8 km at night. At the end of the war, optical telephone communication was tested; special Blinkgerats were used in balloons, aeroplanes, and tanks for communication, with varying degrees of success. After that Carl Zeiss and Jena [18] developed optical speaking devices and they were used in World War II by the German army in anti-aircraft defence units. In 1960, the FSO was revolutionised by laser inventions [19]. FSO was first made available for purchase by Cable Free in 1997 at 62 Mbps and then at 1 Gbps in 1999. The rise of FSO communication was severely constrained by the negative impacts of meteorological conditions, while RF technology more fully met the equivalent requirement for wireless communication. Currently, communication scientists and engineers are faced with the difficulty of finding alternative technology that has a very big bandwidth due to the scarcity of RF spectrum. The greatest choice is optical wireless technology, such as FSO, which offers practically infinite unlicensed bandwidth. FSO has received a lot of interest in research over the past 20 years, and many people are researching in various FSO-related fields. In addition to changing, the FSO is increasing in market value. Although RF systems perform far better in non-LoS conditions, they are more susceptible to interference. As a result, researchers are attempting to combine the two technologies—RF and optical wireless communication, sometimes referred to as hybrid RF/FSO or RF/FSO. When these two technologies work together, they can overcome each other's shortcomings. For example, FSO can get around RF systems' limits and vice versa. The FSO system's finite-area-coverage issue can be solved by the RF component of RoFSO. Some of the WOC market players are- Mostcom, Trimble Hungary, Aoptix Technologies, Optelix, IBSEN telecom, Harris Corporation, Light Pointe Communications, Anova Technologies, Wireless Excellence, FSONA Networks, Mostcom, Cable-free, Mynaric, Skyfibre, and L3 Technologies [20,21]

1.2. Basics of operation

Any communication system transfers. data or information traveling over the air channel from a transmitter at one location to a receiver at another. A laser, a modulator (using a chosen modulation scheme), a laser source driver (to supply the required power supply), and transmitting optics make up the transmitter for an FSO system. The modulator modulates the laser to produce an optical signal by converting bits of information into an electrical signal, depending on the modulation format. In acquisition and tracking contexts, many modulation techniques—such as Q-array Pulse Position Modulation

Page | 2

(PPM), Subcarrier Binary Phase Shift Keying (BPSK), and On-Off Keying (OOK)—have been investigated and compared. In order to minimize diffractive effects that cause the optical beam to spread out and transmit the signal with low directivity, the transmitter optics collimates and extends the beam. The receiver gathers the optical signal as it travels through the air channel in order to recover the data. In the channel, the modulated signal deteriorates. Free space, or air, is the channel that is used in FSO. Rain, fog, and snow all create atmospheric turbulence that scatters, absorbs, and fades broadcast signals, ultimately impairing the functionality of the FSO system. A photodetector, a decoder, and receiving optics make up the receiver. After gathering the optical signal, the receiving optics reduces the beam size such that it fits onto the detector. The detector converts the optical signal back to an electrical signal in order to retrieve the transmitted data [14].

It is crucial to examine FSO performance while taking into account a number of system characteristics. Internal and external parameters are the two groups into which these parameters can be separated. Internal parameters are related to the design of a FSO system and include optical power, wavelength, transmission bandwidth, divergence angle, and optical loss on the transmit side and receiver sensitivity, bit-error rate (BER) [22], receive lens diameter, and receiver field of view on the receiver side. External parameters, or non-system-specific parameters, are related to the environment in which the system must operate and include visibility and atmospheric attenuation, scintillation, deployment distance, window loss, and pointing loss [23,24]. In order to specify the overall performance of the system, several of these characteristics are connected together rather than being independent. Therefore, optimum FSO system design is highly dependent upon the intended application, required availability, and link cost [25,26,27].

1.3. Applications

Space, satellite communication, military applications & terrestrial systems are growing at a fast pace with constant research for better BER and data rates. Unlike RF and satellite communication equipment, laser-based FSOC platforms may be built quickly and efficiently using towers and building support. Major applications of FSOC systems are as listed below [14, 20, 28]:

1. Cellular System Applications: Provides fast data rates to cellular mobile network traffic

2. Military access: FSO is a safe, undetectable and imperceptible framework which connects the link points with low configuration time; hence suitable for military applications of ship to shore/ship, UAVs, aerial, space, satellite-based & land-based terrestrial applications [29].

3. Disaster recovery: FSO can be used as a redundant system for disaster recovery applications including terrorist attacks and natural disaster management as it is rapidly deployable and low cost.

4. Fibre communication reinforcement: Provides reinforcement in case of failure of fibre-based systems

5. Remote Communication: For remotely operating organisations to set-up communication in absence of licence.

6. First and last mile connectivity: Can be used for rapid deployment along with other communication networks as an extension [30].

7. Storage Area Networks: Can be used for integrated and individual block-level data storage.

8. Point-to-Point and Point-to-Multipoint Communication: Between two buildings or two shops or for satellite-to-ground links for short and long-distance communication.

9. Monitoring and video surveillance: FSO supports high-quality video transmission, and hence is an efficient alternative to conventional wireless technology.

1.4. Optical wavelengths

There are multiple transmission windows between the wavelength range of 780 nm and 1600 nm that are almost transparent (attenuation < 0.2 dB/km). These windows are located around several specific centre wavelengths [31,32]:

- 850 nm: This window, which has minimal attenuation, is excellent for FSO operation. Furthermore, it is typically possible to find affordable, high-performing, and dependable transmitter and detector components. In this atmospheric window, sophisticated vertical cavity surface emitting laser (VCSEL) and highly sensitive silicon avalanche photodiode (APD) detector technologies can be employed.

- 1060 nm: Very low attenuation values are seen in the 1060 nm transmission window. Unfortunately, there are extremely few and usually bulky transmission components available to develop FSO systems in this wavelength range. High-grade transmission components are scarce since telecommunications systems do not specifically employ this window. Even in clear weather, there is atmospheric attenuation of many dB/km in the 980 nm wavelength range.

- 1250 nm: Transmitters operating in this optical wavelength range are uncommon, yet the 1250 nm transmission window offers minimal attenuation. Commercially accessible, lower power telecommunications grade lasers typically operate in the 1280–1310 nm range. But around the 1290 nm wavelength, the atmospheric attenuation sharply increases, making this optical wavelength only sporadically appropriate for the optical free space data transmission systems.

- 1550 nm: Because there are many high-quality transmitter and detector components available in this wavelength range and because the band has minimal attenuation, it is a good choice for free space transmission. High-speed semiconductor laser technology, appropriate for WDM operation and utilized to increase transmission power, is one of the components. Free space optical systems can be developed because of the attenuation qualities and component availability at this range.

1.5. Advantages

Owing to different merits and advantages, the FSOC technology has gained huge interests. It can be deployed rapidly to obtain high-speed data connectivity in wireless applications at tough and remote geographical locations, hills & high altitudes where RF systems and optical fibres both options are inaccessible and expensive [33]. Low loss transmissions are achieved by using highly focused and directional laser beams. Therefore, FSOC systems are used for applications such as last-mile connectivity, biomedical applications, military applications, Metropolitan Area Network (MAN), and are chosen for short-range high-data-rate wireless communication. disaster management, etc. The major advantages of FSOC systems can be summed up as follows: [31] [33,34,35,36]:

1. Use of directional and narrow beam width laser at the transmitter gives increased security for transfer of legal, financial, military and other sensitive information

2. Enhanced channel capacity (huge modulation bandwidth capability)

3. Lower installation costs compared with fibre networks or RF systems

4. Immunity from EMI/EMC due to the photonic nature of the signal, hence cannot be detected using RF metre or spectrum analyser. It also offers electric isolation.

5. Use of invisible and eye safe laser beam; environment friendly and clean technology

6. Licence free long-range operation, no frequency allocation/spectrum regulation required

7. Lower installation time frame, flexible and rapid deployment, easy maintenance

8. The deployment of the current system to a different site can be accomplished with ease, since one of the main requirements is the formation of an unimpeded line of sight.

9. Highly focused beam provides almost negligible multipath propagation, and therefore there is reduced fading effects.

10. Flexible topology with scalability

11. . Improved interoperability/transparency while the underlying transmission mechanisms remain unchanged.

12. The FSO system's Mean Time Between Failure (MTBF) is significantly better than that of the RF system.

13. Excellent power focus on the intended receiver due to low power consumption and a short beam divergence angle.

14. Use of lightweight and compact equipment

1.6. Challenges

The atmosphere has a significant impact on FSO performance. This is the greatest challenge as the FSO channel properties will never remain fixed. The main limiting factors of FSO for terrestrial applications are [31, 37, 38,39]:

1. Climatic factors including rain, dust particles, haze, clouds, fog, mist, precipitation and snow lead to attenuation and dispersion [40] [41].

2.   Atmospheric disturbances such as pressure and temperature fluctuations (scintillations) lead to changes in refractive index causing link impairments and beam spreading [42][43].

3.   Physical obstructions such as tall structure, birds, and tall trees can lead to hindrance in the line of sight of transmission blocking the useful signals [44].

4.   Because of Absorption and Scattering during beam propagation it results in signal loss, degradation and reduction in overall system performance.

5.   While making selection of frequency, eye safety should be considered.

6.   Building sways lead to pointing error between transmitter and receiver [45][46].

7.   Signal noise is introduced by solar background radiation, particularly when the signal beam is parallel to the sun rays

8.   Beam spreading cause attenuation of optical beams leading to reduction in received signal power [47].

9.   Ambient noise degrades the FSO link range

This paper has been divided into various sections. Section 2 elaborates comprehensively the Gaussian beam divergence and collimation, what are the causes for beam divergence, and enumerates some of the experimented mitigation techniques available in literature. Section 3 explains the background mathematics and basics of Gaussian beam propagation. Section 4 is the simulation output of Gaussian Beam simulator and MATLAB result that confirms the Gaussian beam propagation formulas related to optimum beam propagation and focusing. Section 5 concludes the paper.

2.   GAUSSIAN BEAM DIVERGENCE AND COLLIMATION

Typically, the laser beam diverges with a noticeably large angle when it exits the fiber and enters open space. The atmospheric conditions are of great importance and should be taken into consideration when a real FSO system is studied. The fundamental transverse electromagnetic mode of a circular laser beam has a Gaussian profile and a spherical wavefront. But in reality, lasers are never truly Gaussian in nature (although He-Ne and Ar-ion lasers are nearly Gaussian). Thus, understanding basic properties of Gaussian beams is important to analyse a real-life laser application. A field that is homogenous, isotropic, and source-free is called free space. A paraxial wave, or almost unidirectional wavefront normal along the propagation axis, is a Gaussian beam propagating in free space. Most laser applications also need a focused, modified or a specified diameter of laser beam waist at a particular location. We can achieve this beam shaping using lenses, beam expanders and other similar optical elements. To minimise divergence in FSO applications and to increase the possible link range, minimising the effect of beam spread, using a collimating lens that is appropriate and situated at the beam's focal length from the transmitting fiber endpoint, we collimate the beam. The beam is focused back onto the fiber by a comparable lens located close to the receiving fiber end point.

Typically, the laser is positioned at the collimating lens's focal point in order to collimate the laser beam [48]. Beam forming optics can be used in long-range fiber optic communications to gather and refocus light fields from optical sources by directing the light in specific directions. A collimated beam is created at the source using a combination of converging and diverging lenses. Figure 1 depicts a basic form of beam collimation that is frequently utilized in long-distance communications. The optical light must emerge over a broader angle for short-range communications to achieve omnidirectionality, but this comes at the cost of a rapid beam expansion with distance. The light source is focused to a point by the converging lens and expanded to a perfect beam by the diverging lens during the ideal collimation process. Instead, in actuality, the source field is concentrated at a single point, and the enlarged beam propagates with a planar beam diameter.

D_L given by

$$D_L = D_0 \left[1 + \left(\frac{2\theta_0 L}{D_0} \right) \right]^{1/2} \tag{1}$$

where D_0 is the output lens diameter, L is the distance from the lens, and θ_0 is the transmitter beam angle. The emerging light appears to uniformly exit over the entire lens at sites in the near field when the collimation diameter is equal to the lens diameter. The beam diameter in the far field increases with distance, giving the impression that light is coming from a single source.
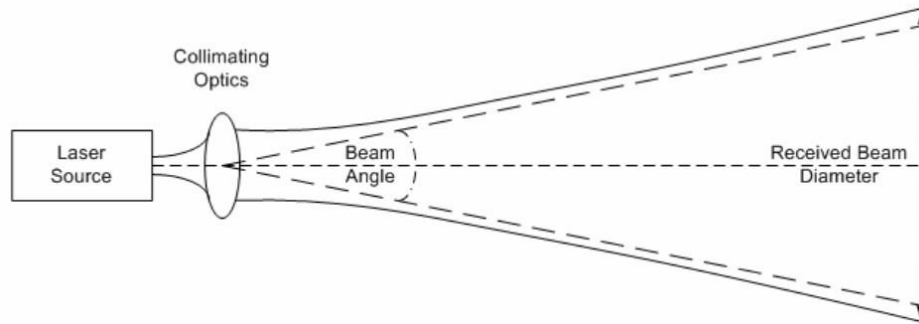
Fig. 1: Beam collimation in long-range propagation [49].

2.1. Causes for beam divergence

The three main atmospheric processes—scattering, absorption, and refractive index variations, or optical turbulence—that impact optical wave propagation in free space are these three.

Absorption and scattering by the constituent gases and particulates of the atmosphere give rise primarily to attenuation of the laser beam [50]. Optical turbulence leads to receiver intensity fluctuations, beam broadening, beam wander, and beam break up [51][52].

When a photon of radiation is received by a gaseous atmosphere molecule, it either reradiates the photon or transforms it into kinetic energy. Therefore, one way that the environment is heated is by absorption. The strongest absorption happens at UV wavelengths, and atmospheric absorption is a strong function of wavelength.There is also a substantial wavelength dependence in light scattering. Smaller-than-wavelength particles, such as air molecules or haze, will result in symmetrical angular distribution of Rayleigh scattering. Rayleigh scattering is highly observable at UV and visible wavelengths, and virtually nonexistent at wavelengths longer than 3 µm. Mie scattering refers to scattering by particles that are similar in size to the wavelength, while geometrical optics can explain scattering by particles that are significantly larger than the wavelengths, such as water droplets. This kind of scattering is more concentrated in the forward direction than Rayleigh scattering.

Other significant optical impacts on a laser beam in propagation are typically temperature differences that show up as fluctuations in the refractive index, or optical turbulence. Temperature variations are almost the only source of these index of refraction fluctuations in the visible and near-infrared sections of the spectrum; humidity fluctuations may also play a role in the far-infrared area. There is a correlation between variations in temperature and pressure and variations in the index of refraction.

2.2. Some available systems for spot size optimization in FSO

In [53], the effect of transmitter beam size on the performance of FSO systems has been determined experimentally. A combination of air scintillation and beam wander generated pointing errors are taken into account in order to find the ideal beam size that minimizes the system's bit error rate (BER). And it is depends on the propagation geometry and turbulence profile.

In [54], for a given atmospheric and misalignment fading statistics, an optimum beam width is selected which maximizes the outage capacity. The FSO system is designed with both capacity and beam width optimization taken into account.The optimum beam width is a function of the outage probability and the average transmitted optical power.

In [55], they propose an adaptive beam control technique for high-altitude airborne platforms interconnected using free-space optical communications (FSOCs), where the beam sizes at both transmitter and receiver are adjusted optimally for the outage probability in the presence of both Angle of Arrival (AoA) fluctuation and pointing error. Use of a focus-tunable lens is proposed to modify the system's focal length without shifting the optical components' positions.

In [56], an adaptive beam control technique combined with beaconless PAT system using variable focus lens is presented. Changing the focal length increases the beam's size and, by modifying the beam divergence angle to suit the link's circumstances, lessens the negative consequences of pointing faults. The amount of aiming error and receiver size affect the ideal beam size at the receiver.

3.   BACKGROUND MATHEMATICS

The fundamental transverse electromagnetic mode (*TEM*$_{00}$) of a circular laser beam has a Gaussian profile and a spherical wavefront. But in reality, lasers are never truly Gaussian in nature (although He-Ne and Ar-ion lasers are nearly Gaussian) [57]. Thus, understanding basic properties of Gaussian beams is important to analyse a real-life laser application. A field that is homogenous, isotropic, and source-free is called free space. A paraxial wave, or virtually unidirectional wavefront normal along the propagation axis, is a Gaussian beam that propagates in free space. Most laser applications also need a focused, modified or a specified diameter of laser beam waist at a particular location. We can achieve this beam shaping using lenses, beam expanders and other similar optical elements.

3.1. Gaussian beam theory

At the transmitter (z = 0), the Gaussian beam propagating along the z axis can be identified by the wave number k = 2π/λ (where λ is the wavelength), the beam spot radius w0, at which the optical intensity falls off to the 1/e2 of the maximum on the beam axis, and the radius of curvature F0, which indicates the beam forming. The beam shapes that are collimated, convergent, and divergent are represented by the situations F0 = ∞, F0 > 0 and F0 < 0. These parameters are usually used to describe the beam at a given position *z = L* by the input-plane beam parameters [58,59].

$$\Theta_0 = 1 - \frac{L}{F_0} \qquad\qquad\qquad (2)$$

$$\Lambda_0 = \frac{2z}{(kw_0^2)} \qquad\qquad\qquad (3)$$

The Fresnel ratio at the input plane is represented by Λ0, whereas the curvature parameter is represented by Δ0. In a similar vein, the input-plane beam parameters and the output plane beam parameters can be defined as

$$\Theta = \frac{\Theta_0}{(\Theta_0^2 + \Lambda_0^2)} = 1 - \frac{L}{F} \qquad\qquad\qquad (4)$$

$$\Lambda = \frac{\Lambda_0}{(\Theta_0^2 + \Lambda_0^2)} = \frac{2L}{(kw^2)} \qquad\qquad\qquad (5)$$

where *F* is the radius of curvature at the receiver. Θ is the refraction parameter and Λ is the diffraction parameter at the output plane. The beam spot radius at the receiver can be expressed by using (2),(3), (4) and (5) as

$$w_z = w_0(\Theta_0^2 + \Lambda_0^2)^{1/2} \qquad\qquad\qquad (6)$$

By using (2) and (3), we can rewrite w_z in terms of distance z as

$$w_z = w_0(\Theta_0^2 + \Lambda_0^2)^{1/2} \qquad\qquad\qquad (7)$$

Beam radius (w_z) is defined as the radial distance where the beam intensity drops by the factor of

$1/e^2 \approx 0.135$ from its peak value. 86.5% of the power is carried within a circle of radius w_z. Beam radius is also equal to the distance (in transverse direction) at which the field amplitude decays to $1/e$ of its maximum value. The waist diameter $2w_0$ is called the beam waist spot size.

Far from the beam center, the beam radius increases approximately linearly with z, defining a cone with half-angle θ0. The angular divergence of the beam is defined by the angle
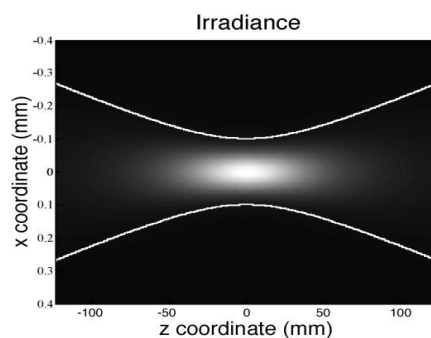

Fig. 2: Irradiance distribution of a Gaussian beam. The bright spot is beam waist [59].

$$\theta_0 = \frac{\lambda}{\pi \omega_0} \qquad\qquad (8)$$

where w0 is the spot size radius at the beam waist. From the equation (8), we see that the divergence and the waist width are reciprocal parameters. Therefore, θ0 does not accurately represent the of the beam close to the beam waist, but as it gets farther away from the beam waist, it gets more precise. A greater divergence angle is produced by a big beam waist, whereas a smaller divergence angle (or more collimated beam) is produced by a tiny beam waist. Thus, it can be said that a When the beam is wide, good collimation (extremely low value of the divergence) is achieved. Regarding On the other hand, permitting a wide divergence angle will result in a highly concentrated beam. In the far-field, the Gaussian beam diffracts with a constant diffraction angle. Since $z \gg z_R$, the spot size for the field amplitude of a Gaussian beam having a waist equal to w_0 propagating in the far field will be a simplified relation between the waist size and the beam spot size at the far-field distance. Thus, for far-field propagation, the beam spot size given by equation (7) becomes

$$w_z \approx \frac{w_0 z}{z_R} = \frac{z\lambda}{\pi w_0} \qquad\qquad (9)$$

Figure 3 demonstrates a Gaussian beam that is released into free space from an optical fiber core. The beam waist is located near the end of the fiber core, as this image illustrates. This figure displays the divergence θ0, beam radius wz, and Rayleigh range zR.. By using equation (8) we may state that if we have a fiber core with radius equal to $5\mu m$ emitting a light of wavelength 1550nm, then the beam divergence will be about $20°$. For this small aperture of beam emission, D. Marcuse [60] proposed the beam waist coincides with the end of core fiber radius *a* and fiber V number in a step-index single-mode fiber:

$$\frac{w}{a} = 0.65 + \frac{1.619}{V^{1.5}} + \frac{2.879}{V^6} \qquad\qquad (10)$$

where $V = \frac{2\pi a}{\lambda} NA$, and *NA* is the fiber numerical aperture. The equation is commonly used for the

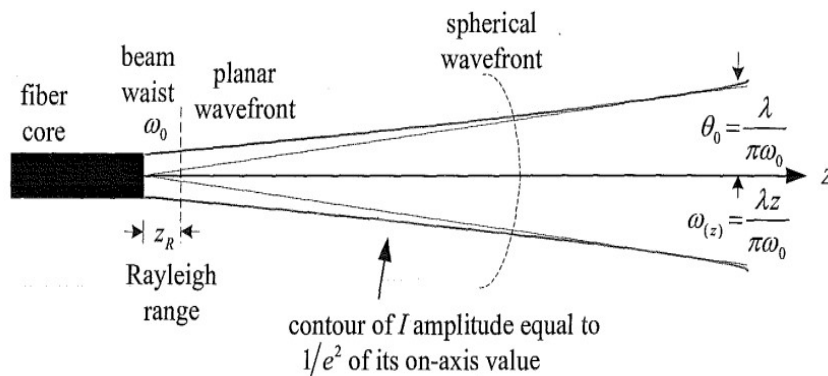Gaussian spot size calculation in step-index single-mode fibers [61].

Fig. 3: Gaussian beam propagating from a fiber core to free space [27]

3.2. Rayleigh range

For some purposes, the speed at which a perfect Gaussian beam will expand as a result of diffraction spreading as it moves out from the waist region must be known. The beam's travel distance from the waist to the point when the beam area spot size doubles i.e., $w = \sqrt{2}w_0$ is called the Rayleigh range of a beam. In the case of a collimated beam, the Rayleigh length forms a dividing line between the near-field (Fresnel region) and the far-field (Fraunhofer region) [62].

$$z_R = \frac{kw_0^2}{2} \qquad\qquad (11)$$

At z = zR, the radius of curvature exhibits its maximum curvature, or minimal value. As the width increases, so does the waist's axial size (with a quadratic dependence). The region of collimation expands when the beam waist's axial extension is increased, leading to improved collimation. more extended. Thus, the maximum Rayleigh range is found in a collimated

beam. The beam splits into two directions. equally by the divergence half-angle θ on both sides of the beam waist. The confocal parameter b is the total distance between the Rayleigh range spot sizes from the beam waist point if a Gaussian beam is focussed from an aperture down to a waist and then expands again. Figure 4 displays the confocal parameter and Rayleigh range of a Gaussian beam.

The Rayleigh range is connected to the Gaussian beam characteristics, which are given as beam radius, curvature radius, and phase retardation.

$$w_z = w_0 \sqrt{1 + \left(\frac{z}{z_R}\right)^2} \qquad (12)$$

$$R_z = z \sqrt{1 + \left(\frac{z_R}{z}\right)^2} \qquad (13)$$

$$\zeta_z = \tan^{-1}\left(\frac{z}{z_R}\right) \qquad (14)$$

The phase retardation of a Gaussian beam range is from $-\pi/2$ at $z = -\infty$ to $+\pi/2$ at $z = \infty$

3.3. Beam collimation using a lens

If a Gaussian beam emits through a set of circularly symmetric thin lenses along the beam axis, then the amplitude distribution remains Gaussian, as long as the overall system maintains a paraxial wave [51]. Sidney Self [63] shows a method to model transformations of a laser beam through simple positive optical
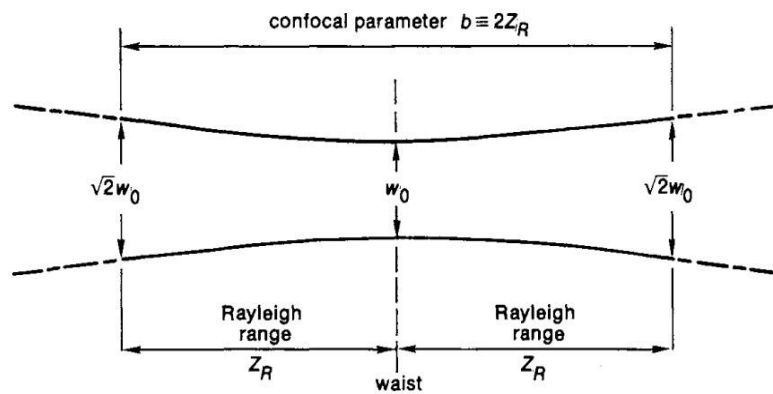

Fig. 4: Rayleigh range and confocal parameter of a Gaussian beam [62]

lens under paraxial conditions, by calculating the Rayleigh range and beam waist location following each individual optical element. These values are computed by a formula similar to the widely used standard lens formula.

The standard lens equation is written as

$$\frac{1}{s} + \frac{1}{s''} = \frac{1}{f} \qquad (15)$$

where f is the lens's focal length, s" is the image distance, and s is the object distance. An analogous formula has been derived for Gaussian beams by assuming that the picture is represented by the output beam's waist and the object by the input beam's waist. The input beam's Rayleigh range is used to express the formula. Gaussian propagation through a narrow lens is depicted in Figure 5.

$$\frac{1}{s + \frac{z_R^2}{(s-f)} + \frac{1}{s''}} = \frac{1}{f} \qquad (16)$$

In the dimensionless form,

$$\frac{1}{\left(\frac{s}{f}\right) + \frac{\left(\frac{z_R}{f}\right)^2}{\left(\frac{s}{f}-1\right)}} + \frac{1}{\left(\frac{s''}{f}\right)} = 1 \qquad (17)$$
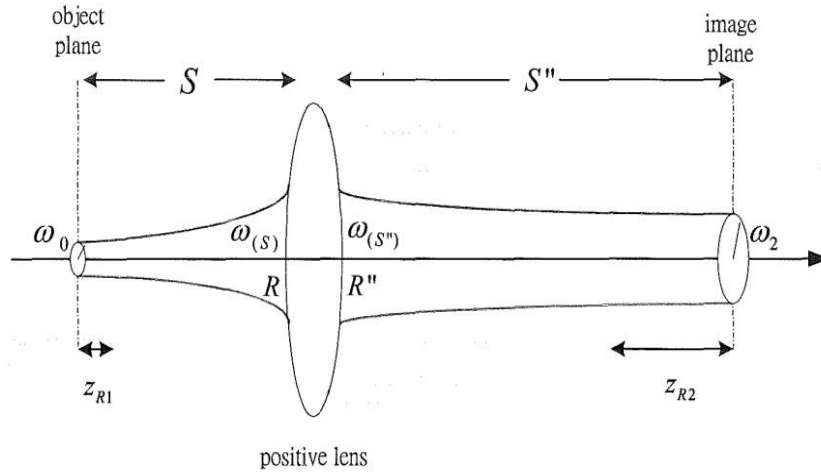
Fig. 5: Gaussian beam propagation through a thin lens [51]

Under paraxial condition, if the input beam waist radius m0 and the object distance S are specified, then the Rayleigh range z_{R1}, the beam's radius w_s, and radius of curvature R at the lens can be calculated from Eq. (11), (12), and (13) respectively. For a thin lens, the beam radius is not changed through the lens $w_s = w_s$, while the radius of the curvature is changed by an amount of ($1/f$) as in the geometrical optics case.

$$\frac{1}{R} + \frac{1}{R''} = \frac{1}{f} \qquad (18)$$

where R" is negative because the transmitted beam's wavefront is converging, and R is positive because the incident beam's wavefront is diverging. The magnification m is given as:

$$m = \left(\frac{w_2}{w_0}\right) = \sqrt{\frac{1}{\left(1-\frac{s}{f}\right)^2 + \left(\frac{z_R}{f}\right)^2}} \qquad (19)$$

The Rayleigh range of the output beam is then given by

$$z_R = m^2 z_R \qquad (20)$$

Figure 6 displays a plot of (s/f) vs (s''/f) for a range of (zR/f) values. This image demonstrates that all curves have a single continuous branch that passes through the same point (s/f) = (s''/f) = 1 for nonzero values of (zR/f). This indicates that, contrary to the geometric optics description, when an item is positioned at the focal length, the image will appear at the opposite side of the focus length. Furthermore, this is not influenced by the ratio (zR/f). Alternatively, for a Gaussian beam waist, since the incident light is at the front focal length of a positive thin lens, then the emerging beam has a waist at the back focal length [64]. Figure 6 is the plot of the lens formula for Gaussian beams.

 -When (s/f) = 1 + (zR/f), it is obvious that (s''/f) has a maximum value of 1 + (zR/2f).

-√ The highest value of the image distance is s" = f + (f 2)

-When s = f + zR, /2zR).

-When (s/f) = 1 − (zR/f), the minimal value of · (s''/f) is 1 − (zR/2f).

- When $s = f - z_R$, image distance $s'' = f + (f^2/2z_R)$

-The maximum magnification is (f/z_R), when object beam waist is at focal length, $s = f$.
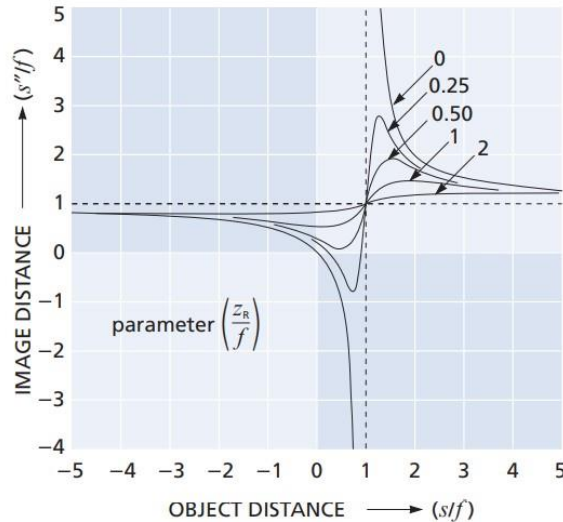
Fig. 6: Plot of the lens formula for Gaussian beams [57]

4.   SIMULATION PLATFORM AND RESULTS

4.1. Gaussian beam simulator

Gaussian beam [65] is an opensource Gaussian optics simulator by Jérôme Lode wyck, written in C++, which provides a table top display of the optical setup and graphically displays the two-dimensional beam propagation characteristics. It also computes the beam parameters with a number of available add-on optics including lenses, flat and curved interfaces, mirrors, dielectric slab and generic ABCD matrix lens. The simulator also has a Magic waist function which finds the suitable arrangement of lenses to achieve the provided target waist diameter. The Fit waist function measures the beam radius or diameter can be used to define the input beam. The simulator also supports save and load configurations of project. The simulation file is saved as an XML document (.xml extension). The output simulation view properties of beam propagation are limited to a maximum height of 10 mm and a maximum width of 10 m. With the help of Gaussian Beam simulator, the maximum input and output beam waist distance calculations are analysed and verified according to the theory.

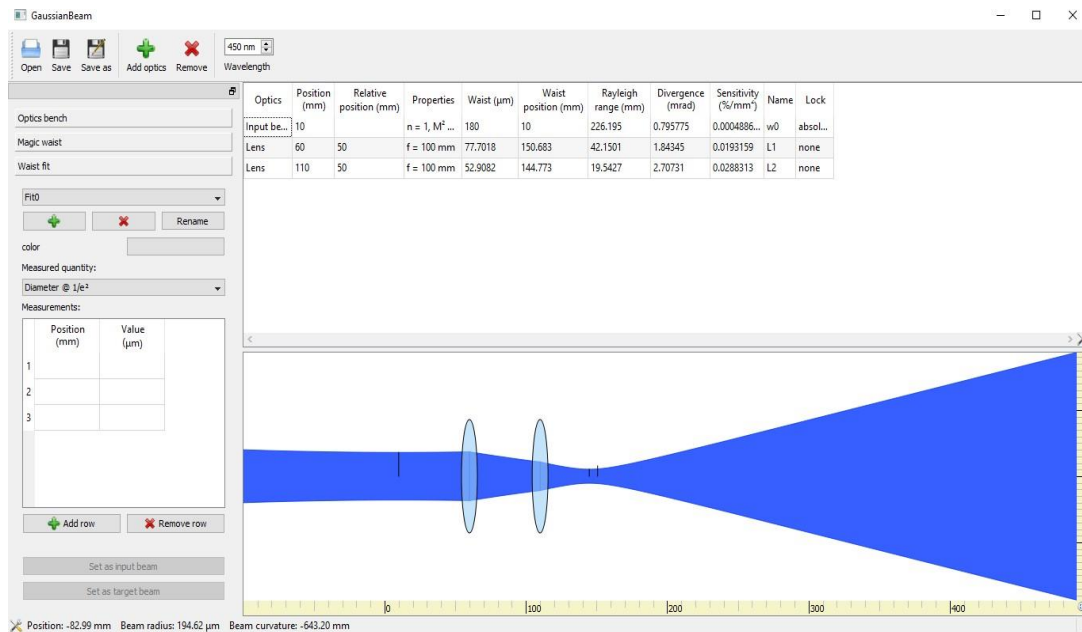**Fig. 7: Gaussian Beam simulator [66]**

Figure 7 shows the first page of a newly created project in the Gaussian Beam simulator. The toolbar at the top has the functions to open a new project, save the current project, add or remove optics and to set the source beam wavelength. To the left, the optics bench boundaries, magic waist adjustment to find the optimum lens positions for achieving the targeted

beam waist and Waist fit functions can be set. For an input beam, the source position, beam propagation parameter (M^2), waist radius, waist position, Rayleigh range, divergence and reference name can be set. The parameters are mathematically connected to each other, hence adding a variable value in the permissible range automatically calculates the related parameter. The source position can also be locked at an absolute position or relative to the added optics. Similarly, any added optics can be set with respect to its individual position on the transmission axis, relative position with respect to the source, focal length of the lens, output beam waist radius, output waist position, Rayleigh range, divergence, reference name, etc. For an input beam of 450 nm wavelength, placed at 0 mm position on the axis with a $40\mu m$ beam waist radius, it calculated a Rayleigh range of 11.1701 mm and divergence equal to 3.58097 mrad. Also a convex lens of focal length 200 mm is placed on the transmission axis. The following observations were made:

1. When the distance between the source beam waist and the lens is equal to the focal length of the lens ($s = f = -200\ mm$), the output beam waist is formed at the back focal length ($s" = f = +200$ mm). The output Rayleigh range is 3580.99 mm and is the maximum possible Rayleigh length at the output. This shows that the beam is collimated when the source is placed at the focal length of the lens. The beam waist size is the largest at this position and the beam spot at the end is comparatively smaller in diameter than any other possible lens positions due to the achieved collimation. Figure 8 shows the simulation output when the beam source is at focal point of lens.

Optics	Position (mm)	Relative position (mm)	Properties	Waist (µm)	Waist position (mm)	Rayleigh range (mm)	Divergence (mrad)	Sensitivity (%/mm²)	Name	Lock
Input be...	0		n = 1, M² ...	40	0	11.1701	3.58097	0.200367	w0	absol...
Lens	200	200	f = 200 mm	716.197	400	3580.99	0.2	0.201619	L1	none

Fig. 8: Laser source at the focal point of lens [66]

2. When the distance between the source beam waist and the lens is less than focal length of the lens ($s < f$, $s = 180\ mm$), the output beam waist is formed at some negative axis point towards the source. ($s" = -1144.47$ mm). The output Rayleigh range is reduced to 851.427 mm generating a less collimated or diverging beam that leads to a bigger beam spot at the end. Figure 9 shows the simulation output when the beam source is at a position less than the lens focal length.

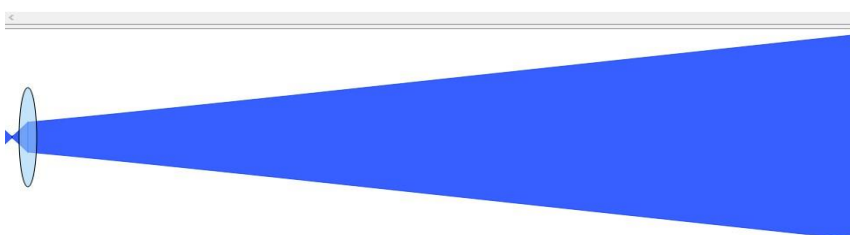| Optics	Position (mm)	Relative position (mm)	Properties	Waist (µm)	Waist position (mm)	Rayleigh range (mm)	Divergence (mrad)	Sensitivity (%/mm²)	Name	Lock
Input be...	0		n = 1, M² ...	40	0	11.1701	3.58097	0.200367	w0	absol...
Lens	180	180	f = 200 mm	349.225	-1144.47	851.427	0.410164	0.197644	L1	none

Fig. 9: Laser source at a position less than the lens focal length [66]

3. When the distance between the source beam waist and the lens is less than focal length of the lens $(s < f$, $s = 180\ mm)$, the output beam waist is formed at some negative axis point towards the source. $(s" = -1144.47\ mm)$. The output Rayleigh range is reduced to 851.427 mm generating a less collimated or diverging beam that leads to a bigger beam spot at the end. Figure 9 shows the simulation output when the beam source is at a position less than the lens focal length.

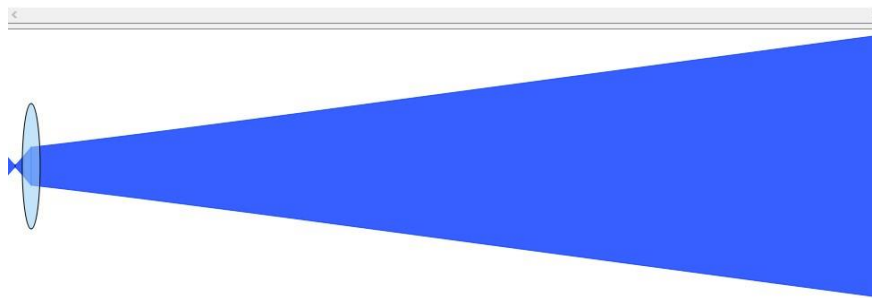| Optics	Position (mm)	Relative position (mm)	Properties	Waist (μm)	Waist position (mm)	Rayleigh range (mm)	Divergence (mrad)	Sensitivity (%/mm²)	Name	Lock
Input be...	0		n = 1, M² ...	40	0	11.1701	3.58097	0.200367	w0	absol...
Lens	180	180	f = 200 mm	349.225	-1144.47	851.427	0.410164	0.197644	L1	none

Fig. 10: Laser source at a position less than the lens focal length [66]

4. when the focal length of the lens is greater than the distance between the source beam waist and the lens $(s > f$, $s = 225\ mm)$, the output beam waist is formed at $(s" = 1758.74\ mm)$. The output Rayleigh range is 595.921 mm, again generating a less collimated or diverging beam that leads to a bigger beam spot at the end. Figure 10 shows the simulation output when the beam source is at a position more than the lens focal length.

Optics	Position (mm)	Relative position (mm)	Properties	Waist (μm)	Waist position (mm)	Rayleigh range (mm)	Divergence (mrad)	Sensitivity (%/mm²)	Name	Lock
Input be...	0		n = 1, M² ...	40	0	11.1701	3.58097	0.200367	w0	absol...
Lens	225	225	f = 200 mm	292.163	1758.74	595.921	0.490272	0.195426	L1	none
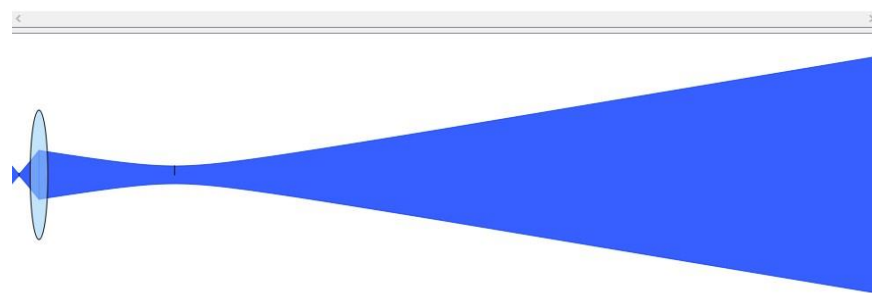
Fig. 11: Laser source at a position more than the lens focal length [66]

5. The maximum image distance till which the output beam waist can travel is obtained when the distance between the lens and the input beam waist is f + zR.. Here, when $(s = 211mm)$, the output beam waist was at the maximum theoretically possible distance (s" = 2201.28 mm). Any variation in the lens position at the either sides from this distance shifted the output beam waist back towards to the lens. Figure 11 shows the simulation of the maximum achievable beam waist position

Optics	Position (mm)	Relative position (mm)	Properties	Waist (µm)	Waist position (mm)	Rayleigh range (mm)	Divergence (mrad)	Sensitivity (%/mm²)	Name	Lock
Input be...	0		n = 1, M² ...	40	0	11.1701	3.58097	0.200367	w0	absol...
Lens	211	211	f = 200 mm	510.299	2201.28	1817.97	0.280697	0.200412	L1	none

Fig. 12: Maximum achievable output beam waist position [66]

4.2. MATLAB calculations

1. A MATLAB code was generated to investigate the beam waist shift in optimum focusing of Gaussian beams as in [66]. For near-field applications, these formulas for optimum focusing of Gaussian beams are valid. Optimization can be done with respect to the lens focal length (f), input beam waist to lens spacing (s), target plane to lens spacing (L), input beam waist radius (w_0) or the source wavelength (λ). Using the formulas for input beam waist to lens spacing (s) optimization, keeping f, L, w_0, λ constant, the value of s for optimum focusing was calculated for a link length of 10 km. The output was equal to the focal length of the lens proving that for long distance propagation, $s = f$ is the best optimized distance between source beam waist and the lens. Figure 12 shows the output window of the MATLAB code for optimum focusing of Gaussian beam.

CODE:

```
clc;

clear all;

close all;

%%

%Input parameters

lambda = 670;               %lambda = Wavelength of laser in nm

f = 200;                    %fl = Focal length of lens in mm

w0 = 3;                     %w0 = Beam waist diameter of laser in mm

L = 10000;                  %z = Distance to find beam spot diameter at in m

%%

%convert into correct units

lambda = lambda * 1e-9; f = f * 1e-3;

w0 = w0 * 1e-3;

%%

s = 1/((1/f)-(1/L));

zr = (pi * w0^2) / lambda;          %zr = Laser rayleigh length

w1 = w0 * sqrt(1+(s/zr)^2);              %Beam radius immediatey in front of lens
```

```
N1 = w1^2/(lambda*L);              %Fresnel number w1

N2 = w0^2/(lambda*(s-f));          %Fresnel number w0

s_ = f + ((L-f)/(1+(pi^2*N2^2)));

wt_ = w0*abs(L/s);

w0_ = wt_/(sqrt(1+(pi^2*N2^2)));

delL = (s_ - f)*(pi^2*N2^2);

%%

%Print output

fprintf("Fresnel Number N1: %f \n", N1)

fprintf("Fresnel Number N2: %f \n", N2)

fprintf("Input beam waist location s: %f m \n", s)

fprintf("Output beam waist location s': %f m \n", s_)

fprintf("Beam waist diameter immediately in front of lens w1: %.8f m \n", w1)

fprintf("Beam waist diameter of output beam w0': %.8f m \n", w0_)

fprintf("Rayleigh range of input beam zr: %f m \n", zr)

fprintf("Beam diameter at L = %f m is wt' = %.8f m \n", L, wt_)

fprintf("Waist shift DeltaL: %f m \n", delL)

fprintf("\n--------------------------------------\n")
```

```
Command Window
    Fresnel Number N1: 0.001343
    Fresnel Number N2: 3358141.791051
    Input beam waist location s: 0.200004 m
    Output beam waist location s': 0.200000 m
    Beam waist diameter immediately in front of lens w1: 0.00300003 m
    Beam waist diameter of output beam w0': 0.00001422 m
    Rayleigh range of input beam zr: 42.200498 m
    Beam diameter at L = 10000.000000 m is wt' = 149.99700000 m
    Waist shift DeltaL: 9999.799189 m

    --------------------------------------
fx >> |
```
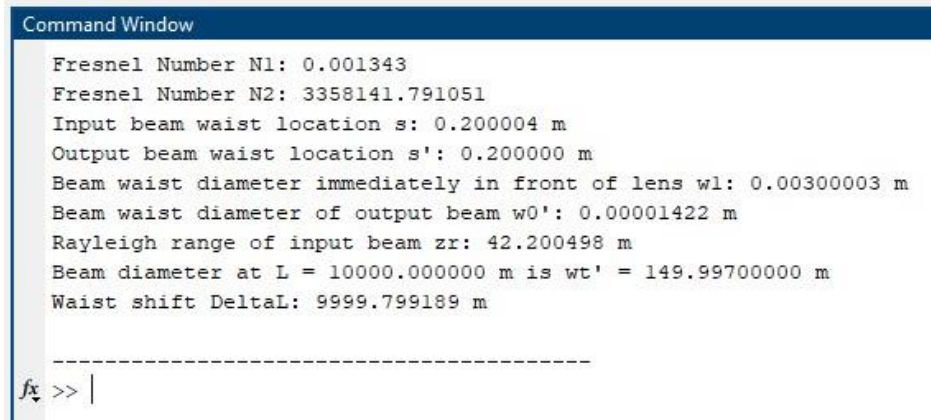
Fig. 13: Beam focusing optimization MATLAB code results

2. A MATLAB code based on the Sidney Self's Gaussian beam focusing formulas was written and the output results were analysed. Increasing the input beam diameter significantly reduced the output spot size of the beam at a far-distant point. Figure 13 shows the output window of the MATLAB code for Sidney Self's Gaussian beam focusing formula.
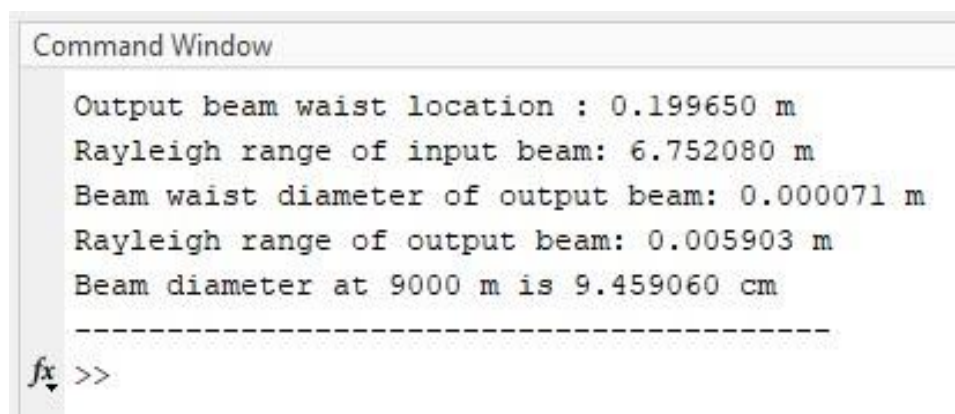
CODE:

clc;

clear all;

close all;

%%

%Input parameters

```
lambda = 670;            %lambda = Wavelength of laser in nm

fl = 200;                  %fl = Focal length of lens in mm

m2 = 1;                  %m2 = Propagation factor

w0 = 1.2;                  %w0 = Beam waist diameter of laser in mm

s = 200;                  %s = Distance between beam waist and lens in mm

z = 9000;                  %z = Distance to find beam spot diameter at in m

%%

%convert into correct units

lambda = lambda * 1e-9;

fl = fl * 1e-3;

w0 = w0 * 1e-3;

s = -s * 1e-3;

%%

%Calculations

alpha = ((m2 * lambda) / pi)^2;

zr = (pi * w0^2) / lambda;

w0_ = (fl * w0) /( sqrt((fl - s)^2 + (w0^4 / alpha)));

zr_ = ((fl * fl) * (w0 * w0)) / (((fl - s)^2 + (w0^4 / alpha)) * sqrt(alpha));

s_ = 1 / ((1 / fl) - (1 / (s + w0^4 / (alpha * (s - fl)))));

wz = w0_ * sqrt(1 + (z/zr)^2);

%%

%Print output

fprintf("Output beam waist location : %f m \n", s_)

fprintf("Rayleigh range of input beam: %f m \n", zr)

fprintf("Beam waist diameter of output beam: %f m \n", 2*w0_) fprintf("Rayleigh range of output beam: %f m \n", zr_)

fprintf("Beam diameter at %d m is %f cm", z, 2*wz*1e2)

fprintf("\n---------------------------------------\n")
```

```
Command Window

    Output beam waist location : 0.199650 m
    Rayleigh range of input beam: 6.752080 m
    Beam waist diameter of output beam: 0.000071 m
    Rayleigh range of output beam: 0.005903 m
    Beam diameter at 9000 m is 9.459060 cm
    ---------------------------------------
fx >>
```

Fig. 14: Sidney Self's beam propagation based MATLAB code results

5. RECENT DEVELOPMENTS IN FSO

The development of free-space optical (FSO) systems has achieved fundamental milestones along with their global implementation [67]. With the rapid advancement and increasing complexity of communication systems, new and sophisticated technologies have emerged. This research paper will detail recent advancements in Free-Space Optical Communication (FSOC) systems, outlining the latest developments and innovations in this field as listed below.

1] RIS assisted RF-FSO communication

2] Communication Performance enhancement using optical amplifier

3] Advance modulation scheme

4] Optical beam position stability controller

5] Advanced error correction algorithm

5.1. RIS assisted RF-FSO communication

I] Recent advancement have led to the development of an RIS-assisted triple- RF-FSO communication technique, which combines Radio Frequency (RF) systems, Free-Space Optical (FSO) communication, and Reconfigurable Intelligent Surfaces (RISs). This innovative approach leverages the strengths of each technology to overcome common challenges and enhance overall communication performance.

In this technique, RISs play a important role in optimizing signal transmission and reception across three distinct stages or hops. The first stage involves transitioning from RF to optical signals, where RISs are integrated into the RF system. The RISs, equipped with programmable surfaces, adjust the phase and direction of the reflected signals, mitigating the effects of signal degradation caused by atmospheric turbulence or environmental factors.

The second hop of the system utilizes RISs in the FSO link. By dynamically adjusting their reflective properties, RISs can correct distortions and compensate for issues such as turbulence and misalignment, which are common in FSO communication. This capability enhances the reliability and clarity of the optical signal as it moves towards the final stage. In the third hop, the system transitions develop a Wireless Optical Communication (UWOC) system underwater. The RISs continue to play a crucial role by optimizing the performance of the UWOC link. Their ability to adjust the optical signal's path and focus helps in overcoming the unique challenges of underwater communication, such as signal attenuation and scattering, ensuring that the signal reaches its intended destination with minimal loss.

One of the key benefits of incorporating RISs in this triple-hop system is their ability to improve performance under varying environmental conditions. Specifically, increasing the number of RIS elements enhances the system's resilience to less turbulent conditions, leading to better overall communication quality. RIS helps to overcome the challenges like a line of sight [68].

II] In the context of smart cities, integrating Reconfigurable Intelligent Surfaces (RIS) with Radio over Free Space Optics (ROFSO) offers a compelling solution to address the challenges of providing reliable 5G services. ROFSO, which combines radio signals with optical communication through the air, faces limitations such as skip zones—areas where signals are weak or non-existent due to obstacles or line-of-sight issues. RIS technology enhances ROFSO by improving signal coverage and quality. RIS surfaces can redirect and amplify optical signals, effectively reducing the impact of skip zones and extending the coverage area. Performance analysis of this integration involves key metrics like outage probability, ergodic channel capacity, and bit error rate (BER). RIS reduces outage probability by enhancing signal strength and reducing the likelihood of performance degradation. It also increases ergodic channel capacity by improving average signal quality and reliability, leading to higher data rates. Additionally, RIS lowers BER by boosting signal strength and minimizing noise, which enhances communication reliability. Heterodyne detection further augments this system by improving signal sensitivity and processing capabilities, making it more effective in detecting weak signals. This integration ultimately results in a more robust and reliable communication system for smart cities, overcoming the limitations of ROFSO and meeting the demands of advanced 5G services [69].

5.2. Communication performance enhancement using optical amplifier

The Free-Space Optical (FSO) communication with advanced optical amplification techniques has emerged as a promising solution. This analysis investigates the effectiveness of wavelength division multiplexing (WDM)-based FSO systems operating at an 80 Gbps data rate, especially in difficult meteorological circumstances.

The study evaluates two primary configurations for optical amplifiers in FSO systems: Amplify-Forward (AF) and Amplify-Received (AR). The performance comparison focuses about Semiconductor Optical Amplifiers (SOA) and Erbium Doped Fiber Amplifiers (EDFA). Simulation results indicate that EDFA significantly outperforms SOA, achieving a maximum optical propagation distance of 1.72 km under strong turbulence. EDFA's superior performance is reflected in its higher optical signal-to-noise ratio (OSNR) of 25.2 dB, a bit error rate (BER) of 2.9×10^{-6}, and a Q factor of 4.5. In contrast, SOA, while simpler and less expensive to install, suffers from higher noise amplification due to factors such as amplified spontaneous emission (ASE) and a higher noise figure (NF), which degrade its performance [70].

The study also explores the use of cascaded optical amplifiers in an Optical Relaying Network (ORN) to extend the optical link distance. Among the amplifiers tested, Raman Amplifiers (RA) demonstrate the most robust performance, extending the optical propagation path to 14.7–15.9 km, even under strong atmospheric turbulence. RAs provide a high signal-to-noise ratio ranging from 24.1 dB to 19.08 dB and a BER between 7.9×10^{-15} and 7.4×10^{-6}, making them highly effective for long-distance communication. In practical implementations, the use of an Optical Band-Pass Filter (OBPF) at the receiver helps mitigate noise and turbulence effects, ensuring cleaner signal detection. The study concludes that while RAs offer the best performance for extended distances, EDFAs are a practical choice for systems requiring moderate performance due to their simpler installation and lower complexity. SOAs, although cost-effective, require additional noise control measures to approach the performance of EDFAs and RAs. This analysis highlights that selecting the appropriate amplifier depends on balancing performance needs with installation complexity and cost considerations [71].

5.3. Advance modulation scheme

In modulation there various advance scheme as listed below:

I] Orthogonal frequency-division modulation (OFDM):

A form of digital transmission called orthogonal frequency-division modulation (OFDM) is used in digital modulation to encode digital (binary) data on many carrier frequencies. Wideband digital communication schemes like OFDM have gained popularity and are now widely utilized in 4G/5G mobile communications, DSL internet access, wireless networks, power line networks, and digital television and audio transmission. The entering bitstream that represents the data to be conveyed in OFDM is split up into several streams. In OFDM the multipath fading effects are reduced. OFDM will provide the high data rate. OFDM cuts the extent of interference in signal broadcasting. Each carrier is modulated with bits from the incoming stream so that multiple bits are delivered in simultaneously. This results in the transmission of numerous closely spaced orthogonal subcarrier signals with overlapping spectra. Fast Fourier transform methods serve as the foundation for the demonstration, and the guard interval added improves orthogonality in transmission channels impacted by multipath propagation. At a low symbol rate, each subcarrier (signal) is modulated using a traditional modulation strategy, such as phase-shift keying or quadrature amplitude modulation. In the same bandwidth, this keeps overall data speeds comparable to traditional single-carrier modulation techniques. The primary benefit of OFDM over single-carrier schemes is its resilience to challenging channel circumstances, such as frequency-selective fading, narrowband interference, and attenuation of high frequencies in long copper wires. because of multipath) without requiring intricate equalization filters. Channel equalization is simplified because OFDM may be viewed as using many slowly modulated narrowband signals rather than one rapidly modulated wideband signal [72].

II] Orthogonal Time Frequency Space Modulation (OTFs):

With the OTFS modulation technique, even in channels with high Doppler or high carrier frequencies (mm-wave), each transmitted symbol experiences a nearly constant channel gain. The temporal and frequency domains of this OTFS signal are well-localized. Mobile radio is a channel that disperses twice. where frequency dispersion is caused by doppler shift and temporal dispersion is caused by multipath propagation phenomenon. Multicarrier signaling methods like OFDM are frequently used to reduce the impact of temporal dispersion-induced inter-symbol interference (ISI). Inter-carrier interference (ICI) caused by Doppler shifts deteriorates the performance of OFDM. The domain of delay-doppler is occupied by the transmitted signal. When the time and frequency domains are in operation, the OTFS waveform does not change. A signal cannot be simultaneously localized in time and frequency due to Heisenberg's uncertainty principle. However, the delay Doppler domain is where the OTFS waveform is confined, and when evaluated in this domain, TDMA and OFDM turn into OTFS limiting instances. The Zak transform is used when transmitting an OTFS waveform in the delay-doppler domain. The Heisenberg Uncertainty Principle will be satisfied by this OTFS since the signal is localized in the delay-doppler form. In the Delay-Doppler domain, it successfully converts the time-varying multipath channel into a 2D channel. With the use of this transformation and equalization in this domain, the channel gain of every symbol is kept

constant during transmission. First, the Delay–Doppler domain information symbols x[k,l] are mapped to symbols X [n, m] to create the time-domain signal s(t), which is then sent over a wireless channel. This is the first step in the modulation process. The time-domain signal r(t) is transferred at the receiving end to the time-frequency domain using the Wigner transform, which is the opposite of the Heisenberg transform. The Delay–Doppler domain is then used for symbol demodulation. The technique is under consideration for networks that use 6G. In terms of transmission, the transmit signals of OTFS in either discrete time sequence or continuous time waveform are the same as that of single antenna vector OFDM (VOFDM) systems [73].

III] Polarization shift keying (POLSK):

signal frequency that decreases over time is called as down chirp and frequency that increases over time is known as up chirp . Chirp OOK signals with mutual inversion and orthogonal X- and Y-polarizations. This modulation method offers strong resistance to laser phase noise and is free from frequency chirp. A signal frequency that rises with time is called a chirp. Combining mutually inverted OOK signals with orthogonal X- and Y-polarizations produced by Mach-Zehnder modulators allowed for the modulation of the POLSK signal. the OOK signal with X-polarization and rotate polarization of bits '1' and '0' according to the nonlinear gain and polarization characteristics. Linear polarizer (LP) with X-polarization is used to invert OOK signal and recover rotational polarization by blocking the polarization of bit '1', since the bit '1' has a significantly bigger magnitude of polarization rotation than bit '0'. Orthogonal X- and Y-polarizations combined with mutually inverted OOK signals yield the POLSK signal. This modulation method does not suffer from frequency chirp and offers strong immunity against laser phase noise. A signal frequency that rises with time is the chirp frequency. Chirp will be present when rising edge of pulse has a slightly different frequency than the falling edge [74].

IV] Orbital angular momentum modulation (OAM):

This modulation system that allows for 10Gbps optical transmission even in the presence of severe air turbulence. This modulation is inexpensive. OAM uses less energy. the transmission of photon data, including frequency, time, phase, amplitude, and polarization, in order to increase photon efficiency while maintaining a reasonable system cost. Photons possess the ability to carry two types of angular momentum: orbital angular momentum (OAM) linked to the azimuthal phase of the complex electric field and spin angular momentum (SAM) connected with polarization. An OAM of $l\hbar$ can be carried by any photon with azimuthal phase dependence of the type $\exp(l\phi\hbar)$ $(l = 0, \pm 1, \pm 2,\ldots)$. The dimensions $N = 2K + 1$ correspond to OAM states $(2K + 1)$. When we increase the number of orthogonal basis function, we increase the aggregate data rate of the system reliable transmission at these high transmission speeds by using LDPC codes at each level [75].

5.4. Optical beam position stability controller

When there is inaccurate beam alignment it led to the significant power loss deteriorate system performance.to remove this misalignment problem there is advanced technologies for improving beam stability and positioning accuracy.We get this data by the quad detector which is Place the sensitive detector in the proper location and produce the necessary outputs to use a quick steering mirror to guide the beam. In the quad detector there are four photodiodes. This detector will measure the position by evaluating the light intensity on each photo diode. This positional data is important to adjust the path using fast steering mirror which provides rapid adjustments to counteract any detected misalignment. To increase the performance of the detector system we use controllers. In the controller we can use either the fizzy or PID controller. The PID is the simple controller which works by adjusting the mirror position based on the error signal, with separate adjustments for the current error (Proportional), accumulated past errors (Integral), and predicted future errors (Derivative). And the fuzzy controller is works by applying "if-then "rule handling uncertainties and non-linearities more flexibly. This makes fuzzy logic controllers particularly useful in complex environments where traditional methods might fall short [76].

There is more recent developments in which we used these two controllers, so basically in the Adaptive optics (Ao) will adjust the shape of light waves to correct distortion. There is three parts in the Adaptive optics which is Wave front corrector, wavefront sensor, control system. wavefront sensors is a device who measures the shape of optical wavefront. in adaptive optics systems is the Shack–Hartmann wavefront sensor. This sensor consists of an array of micro lenses that focus the incoming light onto a detector plane. A central component of an adaptive optics system is the wavefront correction device In Wave front corrector there is one deformable mirror has a substantial number of actuators that can deform the surfaces in various ways to correct a wide range of wavefront distortions. Typically, each actuator of a deformable mirror primarily controls the height elevation of the mirror surface in its immediate vicinity, but it also has some influence on the surface shape further away. Similar phenomena may occur to some extent with other types of corrective devices. The control system

in an adaptive optics setup is in charge of producing control signals for the correction device using the wavefront data that the wavefront sensor has collected. Ideally, it should provide accurate compensation while fully utilizing the speed offered by the correction device [77].

5.5. Advanced error correction algorithm

1. Low density parity-check codes (LDPC) :

The state of the art in contemporary channel coding is represented by the class of low-density parity-check (LDPC) codes. Their near-capacity performance across a wide range of data transmission and storage channels, along with the manageable complexity of their decoders, have drawn the attention of coding theorists and practitioners during the past 10 years. Gallager created them in his doctoral dissertation from 1960, and in the 35 years that followed, they were hardly given any thought. Tanner stands out as one prominent exception. In a seminal study from 1981, Tanner presented a graphical depiction of LDPC codes that is now known as Tanner graphs and generalized LDPC codes. MacKay, Luby, and others redesigned LDPC codes in the mid-1990s, seemingly unrelated to Gallager's work, after realizing the benefits of linear.LDPC codes are designed with block codes that have low-density parity-check matrices. We first explain the EXIT chart technique for determining (near-)optimal degree distributions for LDPC code ensembles, which can be used as a target by the code designer. Additionally, we show how easy it is to express codes using protographs and how this always results in quasi-cyclic LDPC codes. Next, the EXIT chart method is expanded to include protograph-based LDPC codes as a special case. We next go into a number of design strategies, including quasi-cyclic accumulator based codes, for LDPC codes that include one or more accumulators. The study then examines a number of algebraic LDPC code design strategies in its second part. The codes whose designs are based on Reed-Solomon codes are explored after codes based on finite geometries. Codes that are cyclic, quasi-cyclic, and structured result from the algebraic designs. Additionally, the masking technique for generating irregular codes from regular quasi-cyclic LDPC codes is provided. A portion of these codes and findings are unique to this presentation. The binary-input AWGN channel (BI-AWGNC) is the subject of this research. On the other hand, as the study discusses, good BI-AWGNC codes are typically good across a wide range of channels. As an alternative, the reader could use this work as a springboard for further exploration of more complex avenues [78].

2. Bose-Chaudhuri-Hocquenghem codes (BCH):

The BCH code is a sub class of the cyclic codes which is used in communication system. BCH code is one of the error correction algorithm.in the new technology it introduced the minimum distances of the dual codes, particularly improving on existing bounds. BCH codes are characterized by their construction relative to a primitive nth root of unity, denoted as β, in an extension field of Fq.

A particularly interesting subset of BCH codes is known as dually-BCH codes. These are BCH codes whose dual codes are the codes where the generator polynomial's dual is also a BCH code relative to the same primitive root β are themselves BCH codes. Determining whether a BCH code is dually-BCH is a challenging problem due to the complex interplay between the code and its dual. There is two types of BCH codes: Both projective narrow-sense ternary BCH codes and primitive narrow-sense BCH codes. Narrow-sense BCH codes are a special case of BCH codes with specific parameters that simplify their construction and analysis. The paper provides clear criteria based on the designed distance $\delta \backslash$ delta δ of the BCH code to determine whether the code is dually-BCH. Designed distance $\delta \backslash$ delta δ is a measure of the error-correcting capability of the code, with higher values indicating better performance [79].

6. CONCLUSION

Three factors restrict the size of the spot:

1) The wavelength to input beam diameter ratio provides the diffraction limit.

2) The divergence of the laser beam.

3) The spherical aberration of the lens.

You can make changes to this draft to better suit your needs, and you can use Grammarly Free's recommendations to make sure your finished output is exceptional. In order to reduce the impact of signal loss, it is essential to ensure that the receiver aperture is sufficiently large, while keeping the transmitter aperture small and minimizing the angle of laser beam divergence. The optimal size of the transmitter beam is directly influenced by atmospheric conditions and varies significantly based on the geographical location of the link establishment. Employing a beam expander to produce a well-

collimated beam at the transmitter, with a width on the order of centimeters, can facilitate the propagation of a less divergent beam to the far-field. This study delves into recent advancements in Free-Space Optical (FSO) systems, including developments in Reconfigurable Intelligent Surfaces (RIS), optical amplification, modulation, stability control, and error correction algorithms. Through the utilization of devices such as RIS, optical amplifiers, and stability controllers, significant progress has been achieved in enhancing stability, resolving line-of-sight issues, and other related challenges.

REFERENCES

[1] Kerr, J. R., et al. "Atmospheric optical communications systems." *Proceedings of the IEEE* 58.10 (1970): 1691-1709.

[2] Das, Santanu, et al. "Requirements and challenges for tactical free-space lasercomm." *MILCOM 2008-2008 IEEE Military Communications Conference*. IEEE, 2008.

[3] Raj, Arockia Bazil, and Arun K.Majumder. "Historical perspective of free space optical communications: from the early dates to today's developments." Iet Communications 13.16 (2019): 2405-2419.

[4] Raj, A. Arockia Bazil. Free space optical communication: system design, modeling, characterization and dealing with turbulence.Walter de Gruyter GmbH & Co KG, 2015.

[5] Willebrand, Heinz, and Baksheesh S. Ghuman. *Free space optics: enabling optical connectivity in today's networks*. SAMS publishing, 2002.

[6] Kaushal, Hemani, V. K. Jain, and Subrat Kar. *Free space optical communication*. New Delhi: Springer india, 2017.

[7] Majumdar, Arun K., Zabih Ghassemlooy, and A. Arockia Bazil Raj. Principles and applications of free space optical communications .No. 78. The Institution of Engineering and Technology, 2019.

[8] Patle, Nidhi, et al. "Review of fibreless optical communication technology: History, evolution, and emerging trends." Journal of Optical Communications 45.3 (2024): 679-702.

[9] Chowdhury, Mostafa Zaman, et al. "A comparative survey of optical wireless technologies: Architectures and applications." *ieee Access* 6 (2018): 9819-9840.

[10] Khalighi, Mohammad Ali, and Murat Uysal. "Survey on free space optical communication: A communication theory perspective." *IEEE communications surveys & tutorials* 16.4 (2014): 2231-2258.

[11] Willebrand, Heinz A., and Baksheesh S. Ghuman. "Fiber optics without fiber." *IEEE spectrum* 38.8 (2001): 40-45.

[12] Agrawal, Govind P. "Optical communication: its history and recent progress." *Optics in our time* (2016): 177-199.

[13] Holzmann, Gerard J. "Data Communications: The First 2500 Years." *IFIP Congress (2)*. 1994.

[14] Dibner, Bern. "Ten founding fathers of electrical science: Vii. Karl Friedrich Gauss." *Electrical Engineering* 73.10 (1954): 874-875.

[15] Hutt, D. L., K. J. Snell, and P. A. Belanger. "Alexander Graham Bell's Photophone." *Optics and Photonics News* 4.6 (1993): 20-25.

[16] Bell, Alexander Graham. "The photophone." *Science* 11 (1880): 130-134.

[17] Hassan, M. Mubasher, and G. M. Rather. "Free Space Optics (FSO): A promising solution to first and last mile connectivity (FLMC) in the communication networks." *IJ Wireless and Microwave Technologies* 4 (2020): 1-15.

[18] Hagen, Antje. "Export versus direct investment in the German optical industry: Carl Zeiss, Jena and Glaswerk Schott & Gen. in the UK, from their beginnings to 1933." *Business History* 38.4 (1996): 1-20.

[19] Hecht, Jeff. "A short history of laser development." *Applied optics* 49.25 (2010): F99-F122.

[20] Patle, Nidhi, et al. "Review of fibreless optical communication technology: history, evolution, and emerging trends." *Journal of Optical Communications* (2021).

[21] Raj, Arockia Bazil, and Arun K. Majumder. "Historical perspective of free space optical communications: from the early dates to today's developments." *IET Communications* 13.16 (2019): 2405-2419.

[22] Jagdale, Atharva Ninad, and AA Bazil Raj. "Model-Free Ber Measurement in Free Space Laser Communication Link." 2021 International Conference on System, Computation, Automation and Networking (ICSCAN) . IEEE, 2021.

[23] Joseph, C., Kumar, E. S. V., Raj, A. B., & Sharma, N. (2023, December). A Linear Closed Loop Feedback System for Beam Wander Correction in Medium-Range Optical Link. In 2023 IEEE Pune Section International Conference (PuneCon) (pp. 1-5). IEEE

[24] Raj, A. Arockia Bazil, and J. P. Lancelot. "Seasonal investigation on prediction accuracy of atmospheric turbulence strength with a new model at Punalkulam, Tamil Nadu." Journal of Optical Technology 83.1 (2016): 55-68

[25] Bloom, Scott, et al. "Understanding the performance of free-space optics." *Journal of optical Networking* 2.6 (2003): 178-200.

[26] Raj, A. Arockia Bazil, J. Arputha Vijaya Selvi, and S. Durairaj. "Comparison of different models for ground-level atmospheric turbulence strength (Cn_2) prediction with a new model according to local weather data for FSO applications." Applied optics 54.4 (2015): 802-815.

[27] Raj, A. Arockia Bazil, et al. "Design of cognitive decision making controller for autonomous online adaptive beam steering in free space optical communication system." Wireless Personal Communications 84 (2015): 765799.

[28] Ghassemlooy, Zabih, and Wasiu Oyewole Popoola. *Terrestrial free-space optical communications*. London, UK: InTech, 2010.

[29] Majumdar, Arun K., Zabih Ghassemlooy, and A. Arockia Bazil Raj. Principles and applications of free space optical communications. No. 78. The Institution of Engineering and Technology, 2019.

[30] Ghassemlooy, Zabih, Arun Majumdar, and Arockia Bazil Raj."Introduction to free space optical (FSO) communications." (2019): 126.

[31] Alkholidi, Abdulsalam Ghalib, and Khaleel Saeed Altowij. "Free space optical communications—theory and practices." *Contemporary Issues in Wireless Communications* (2014): 159-212.

[32] Arockia Bazil Raj, A., and S. Padmavathi. "Statistical analysis of accurate prediction of local atmospheric optical attenuation with a new model according to weather together with beam wandering compensation system: a seasonwise experimental investigation." Journal of Modern Optics 63.13 (2016): 1286-1296.

[33] Raj, A. Arockia Bazil, et al. "A review–unguided optical communications: Developments, technology evolution, and challenges." Electronics 12.8 (2023): 1922.

[34] Majumdar, Arun K., and Jennifer C. Ricklin, eds. *Free-space laser communications: principles and advances*. Vol. 2. Springer Science & Business Media, 2010.

[35] Kim, Isaac I., and Eric J. Korevaar. "Availability of free-space optics (FSO) and hybrid FSO/RF systems." *Optical Wireless Communications IV*. Vol. 4530. SPIE, 2001.

[36] Kumar, Suresh, and Nishant Sharma. "Emerging Military Applications of Free Space Optical Communication Technology: A Detailed Review." *Journal of Physics: Conference Series*. Vol. 2161. No. 1. IOP Publishing, 2022.

[37] Farooq, Essar, Anupam Sahu, and Sachin Kumar Gupta. "Survey on FSO communication system—Limitations and enhancement techniques." *Optical and wireless technologies*. Springer, Singapore, 2018. 255-264.

[38] Kumar, Naresh, and Ashwani Kumar Rana. "Impact of various parameters on the performance of free space optics communication system." *Optik* 124.22 (2013): 5774-5776.

[39] Raj, A. Arockia Bazil, and S. Padmavathi. "Quality metrics and reliability analysis of laser communication system." Defence Science Journal 66.2 (2016): 175185.

[40] De, Sampurna, and AA Bazil Raj. "Experimental study of sand-storm effect on digital fso communication link." 2020 International Conference on Recent Trends on Electronics, Information, Communication & Technology (RTEICT) . IEEE, 2020.

[41] Raj, A. Arockia Bazil, and J. Arputha Vijaya Selvi. "Comparison of different models for ground-level atmospheric attenuation prediction with new models according to local weather data for FSO applications." Journal of optical communications. 36.2 (2015): 181.

[42] Raj, A. Arockia Bazil, et al."Mitigation of beam fluctuation due to atmospheric turbulence and prediction of control quality using intelligent decision-making tools." Applied optics 53.17 (2014) 3796-3806.

[43] Eguri, Samson Vineeth Kumar, Arockia Bazil Raj A, and Nishant Sharma. "Survey on acquisition, tracking and pointing (ATP) systems and beam profile correction techniques in FSO communication systems." Journal of Optical Communications 0 (2022).

[44] Raj, A. Arockia Bazil, J. Arputha Vijaya Selvi, and S. Raghavan. "Terrestrial free space line of sight optical communication (tfslsoc) using adaptive control steering system with laser beam tracking, aligning and positioning (atp)." 2010 International Conference on Wireless Communication and Sensor Computing (ICWCSC) . IEEE, 2010.

[45] ArockiaBazilRaj, A., and Ucuk Darusalam. "Performance improvement of terrestrialfree space optical communications by mitigating the focal-spot wandering." Journal of Modern optics 63.21 (2016): 2339-2347.

[46] Raj, A. Arockia Bazil. "Mono-pulse tracking system for active free space optical communication." Optik 127.19 (2016): 7752-7761.

[47] Arockia Bazil Raj, A., et al. "A direct and neural controller performance study with beam wandering mitigation control in free space optical link." Optical Memory and Neural Networks 23 (2014): 111129

[48] J. Ning, W. Zhang, C. Cao, Z. Feng, X. Zeng, T. Wang, R. Wang, Q. Song, S. Fan, Collimation of laser diode beams for free space optical communications, Infrared Physics & Technology 102 (2019) 102996.

[49] K.-m. Lo, Design and analysis of optical layouts for free space optical switching (2002).

[50] Raj Anthonisamy, Arockia Bazil, Padmavathi Durairaj, and Lancelot James Paul. "Performance analysis of free space optical communication in open-atmospheric turbulence conditions with beam wandering compensation control." IET Communications 10.9 (2016): 10961103.

[51] H. Sun, Thin lens equation for a real laser beam with weak lens aperture truncation, Optical Engineering 37 (11) (1998) 2906–2913.

[52] Bazil Raj, Arockia A., et al. "Intensity feedback-based beam wandering mitigation in free-space optical communication using neural control technique." EURASIP Journal on Wireless Communications and Networking 2014 (2014): 1-18

[53] H. Kaushal, G. Kaddoum, V. K. Jain, S. Kar, Experimental investigation of optimum beam size for fso uplink, Optics communications 400 (2017) 106–114.

[54] A. A. Farid, S. Hranilovic, Outage capacity optimization for free-space optical links with pointing errors, Journal of Lightwave technology 25 (7) (2007) 1702–1710.

[55] V. V. Mai, H. Kim, Beam size optimization and adaptation for high-altitude airborne free-space optical communication systems, IEEE Photonics Journal 11 (2) (2019) 1–13.

[56] V. V. Mai, H. Kim, Beaconless pat and adaptive beam control using variable focus lens for free-space optical communication systems, APL Photonics 6 (2) (2021) 020801.

[57] C. M. Griot, Gaussian beam optics, Gaussian Beam Opt 2 (1) (2009).

[58] L. C. Andrews, R. L. Phillips, Laser beam propagation through random media, Laser Beam Propagation Through Random Media: Second Edition (2005).

[59] J. Alda, Laser and gaussian beam propagation and transformation, Encyclopedia of optical engineering 999 (2003).

[60] D. Marcuse, Loss analysis of single-mode fiber splices, Bell system technical journal 56 (5) (1977) 703–718.

[61] G. Keiser, Optical fiber communications, Vol. 2, McGraw-Hill New York, 2000.

[62] A. E. Siegman, Lasers, University science books, 1986.

[63] S. A. Self, Focusing of spherical gaussian beams, Applied optics 22 (5) (1983) 658–661.

[64] J. Ã. Brand Faria, Optimal focusing of gaussian beams, Microwave and Optical Technology Letters 4 (8) (1991) 304–307.

[65] Lodewyck, Gaussianbeam, https://sourceforge.net/projects/gaussianbeam/, accessed: 2007-06-22.

[66] Y. Li, J. Katz, Optimum focusing of gaussian laser beams: beam waist shift in spot size minimization, Optical Engineering 33 (4) (1994) 1152–1155.

[67] Darusalam, U., Raj, A. B., Zulkifli, F. Y., Priambodo, P. S., & Rahardjo, E. T. (2023). The relaying network in free-space optical communications using optical amplifiers in cascaded configuration.

[68] Makara Journal of Technology, 27 (2), 3.Kumar, L. Bhargava, et al. "RIS assisted triple-hop RF-FSO convergent with UWOC system." IEEE Access 10 (2022): 66564-66575.

[69] Kumar, Abhishek, Prabu Krishnan, and A. Arockia Bazil Raj. "Performance analysis of a RIS assisted RoFSO communication system over Malaga distribution for smart city applications." Applied Optics 62.19 (2023): 5325-5333.4

[70] Darusalam, Ucuk, et al. "Performance of free-space optical communication systems using optical amplifiers under amplify-forward and amplify-received configurations." Makara Journal of Technology 24.3 (2020):

[71] Darusalam, U., Raj, A. B., Zulkifli, F. Y., Priambodo, P. S., & Rahardjo, E. T. (2023). The relaying network in free-space optical communications using optical amplifiers in cascaded configuration. Makara Journal of Technology, 27 (2), 3.

[72] Khosla, Dishant, et al. "OFDM modulation technique & its applications: a review." International Conference on Innovations in Computing (ICIC 2017). 2017.

[73] Mohammed, Saif Khan. "Derivation of OTFS modulation from first principles." IEEE transactions on vehicular technology 70.8 (2021): 7619-7636

[74] Yan-Qing Hong and Sang-Kook Han, "Polarization-dependent SOA-based PolSK modulation for turbulence-robust FSO communication," Opt. Express 29, 15587-15594 (2021)

[75] Ivan B. Djordjevic and Murat Arabaci, "LDPC-coded orbital angular momentum (OAM) modulation for free-space optical communication," Opt. Express 18, 24722-24728 (2010)

[76] Lahari, Sreerama Amrutha, ArockiaBazil Raj, and S. Soumya. "Control of fast steering mirror for accurate beam positioning in FSO communication system." 2021 International Conference on System, Computation, Automation and Networking (ICSCAN) . IEEE, 2021

[77] Siby, Ashly, Arockia Bazil Raj, and S. Soumya. "Controller design for optical wave-front stabilization in FSO communication system." 2021 international conference on system, computation, automation and networking (ICSCAN) . IEEE, 2021.

[78] https://jcoms.fesb.unist.hr/pdfs/jcomss_v2n3_september2006_191-211.pdf

[79] C. Ding, "Parameters of Several Classes of BCH Codes," in *IEEE Transactions on Information Theory*, vol. 61, no. 10, pp. 5322-5330, Oct. 2015, doi: 10.1109/TIT.2015.2470251.